Hindawi Publishing Corporation
Journal of Nanoscience
Volume 2013, Article ID 586208, 5 pages
http://dx.doi.org/10.1155/2013/586208

Research Article

Distinguishing Field Effects from Charge Effects in the Optoelectronic Properties of Carbon Nanotube Films

W. Joshua Kennedy

Structural Engineering Division, NASA Johnson Space Center, Houston, TX 77058, USA

Correspondence should be addressed to W. Joshua Kennedy; w.joshua.kennedy@gmail.com

Received 2 April 2013; Accepted 12 June 2013

Academic Editor: Changxin Chen

We have used charge-induced absorption to quantify the influence of injected charges on electroabsorption measurements in single-wall carbon nanotube films. The interpretations of experimental measurements of $\chi^{(3)}$ processes in nanotubes are simplified by taking into account the change in electron-electron interactions upon charge injection. Electroabsorption spectra that are properly corrected for charge-induced effects show remarkable agreement with a simple Stark shift of the exciton transitions with no notable second-derivative contributions. Thus, distinguishing electric field effects from carrier density effects allows for a more rigorous calculation of exciton polarizability from electroabsorption measurements, even in heterogeneous films. PACS: 78.67.Ch Nanotubes: optical properties of low-dimensional, mesoscopic, and nanoscale materials and structures.

1. Introduction

While much attention has been given to precise optical measurements on individual single-wall carbon nanotubes (SWNTs) or monodispersed populations of SWNTs, devices made from heterogeneous mixtures of nanotubes continue to be of interest for use as field emitters, actuators and transducers, chemical sensors, transparent conductive films, and field-effect transistors [1–6]. Electroabsorption (EA) is a powerful tool for understanding the nature of excited states in materials, and the technique has been applied to various types of nanotube samples over the course of the last decade. The absence of Franz-Keldysh oscillations in EA spectra of nanotubes was used as evidence of the excitonic nature of the photoexcitations in SWNTs [7–9]. Furthermore, EA spectra have provided a quantitative estimate of exciton polarizability and size in individual species, evidence for charge trapping in SWNT bundles, and evidence for the existence of low-energy "dark" excitons in order to explain the low photoluminescence quantum efficiency in SWNTs [10–12].

Unfortunately, EA spectra of heterogeneous mixtures of SWNTs suffer from a variety of complex interactions. Perturbation of π orbitals due to bundling, intertube charge transfer or trapping, and other competing effects can obfuscate individual tube responses to external fields. Because of these interactions, the analysis of SWNT EA spectra is less straightforward than for many other materials.

Charge-induced absorption (CA) is a complementary technique that elucidates the influence of excess charge carriers independent of photoexcitations. This technique has been used in conducting polymers to measure carrier transport and recombination dynamics and to identify polaron absorption bands [13–15]. In the present work, we show that a common feature in the EA spectra of SWNTs may be attributed to the influence of coincidentally injected charges. We measure the CA and EA spectra for films made from identical SWNT populations and fit the EA spectrum to a combination of the first derivative of the absorption and a modified bleaching signal from the semiconducting tubes in the sample shown in CA.

2. Methods

Both CA and EA involve modulating a bias voltage across the sample and measuring the change in intensity of the transmitted light. CA and EA spectra were obtained using a home-built system consisting of a white light source,

a signal generator and matching transformer or amplifier, a monochromator, and a photodiode detector with a lock-in amplifier as shown in Figure 1. For both experiments, HiPCO tubes from Rice were purified via acid treatment and washed in methanol. They were then dispersed in water using the surfactant sodium dodecyl sulfate (SDS) at a 1 : 1 ratio by weight to inhibit bundling. Then, to make the nonconductive EA films, polyvinyl alcohol (a transparent plastic with no significant electronic interaction with the SWNTs) was added to the solution at a 10 : 1 ratio. Films were then drop-cast onto the substrates described next and dried in a vacuum oven at 120°C for one hour to remove water and surfactant.

The fundamental difference between the two techniques is the electrical conductivity of the sample. For EA, the sample should be highly resistive so that very little current flows and the sample experiences a large electric field. For our EA measurements, the PVA-SWNT film resistivity was more than 6 MΩ cm due to the good dispersion of SWNTs in the PVA matrix. These films were deposited on interdigitated gold electrodes (see Figure 1) with a 15 μm gap atop a transparent sapphire substrate, and EA spectra were obtained by modulating the applied field at a frequency of 1 kHz. This is the highest frequency at which our transformer can maintain high voltage output; at lower frequencies, there is an undesirable amount of $1/f$ noise. The lock-in amplifier was synchronized at twice the modulation frequency because the electroabsorption signal depends on the square of the applied field. The temporal and spatial average of the electric field between the electrodes was as high as 10^7 V/m, but the field actually felt by individual nanotubes depends on their dielectric strength because much of the potential drop occurs in the PVA matrix. This effect is linear in the applied voltage and independent of photon energy, so our qualitative results are unaffected.

Scanning electron microscope (SEM) images of both materials are shown in Figure 2. Films were drop-cast onto polished graphite substrates for imaging, but are otherwise identical to the films used for the spectroscopy. SEM spectra were taken using 2 kV accelerating potential in high vacuum. The sample without PVA (Figure 2(a)) consists of a network of nanotube bundles of varying sizes as in many other similar materials reported in the literature. When PVA is added (Figure 2(b)), the surface of the film obscures the network structure and only a hint of the nanotubes can be seen in the image. It is worth noting that the negative charging under high vacuum in the PVA nanocomposite sample is significantly worse than in the pure nanotube film, confirming the difference in electrical conductivity between the two. We surmise that there are very few percolating electrical pathways within the nanotube network across the composite film.

Raman spectra were obtained on both samples, and the results are shown in Figure 3. The diameters obtained from the radial breathing modes (RBM) in our sample are consistent with average sizes of other HiPCO-produced tubes. The tube diameters range from 0.72 nm to 1.33 nm with a median diameter of 1.13 nm. The very low D-band intensity indicates that the nanotubes are highly purified with few defects. The close similarity in the spectra of the two samples, with no measurable shifts or significant intensity changes, confirms that the nanotubes survive the processing and that the PVA matrix does not interact significantly with the nanotube electronic states. The Raman active modes in the PVA have an insignificant cross-section compared to the resonantly enhanced modes in the SWNT.

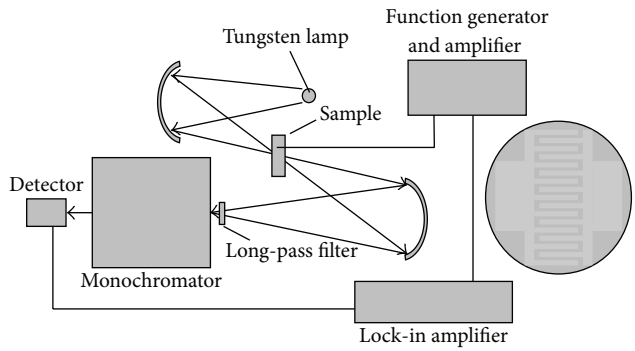

Figure 1: A schematic of the light path and electrical connections for the EA and CA experiments. The figure on the right is a diagram of the interdigitated electrode array with a 15 μm gap between the poles.

For CA measurements, the sample resistivity was 4.3×10^{-3} Ω cm due to good connectivity throughout the SWNT network comprising the film. The conductive films were placed on the same interdigitated electrode array, and a current amplifier was attached to the signal generator and used to drive charges into the films. The mechanism of charge injection in a slightly different configuration has been previously described, and the results were compared to charge injection via electrochemical doping [16]. The gold contacts provide a very low barrier to holes, which are the dominant carriers in undoped SWNTs, but they are very inefficient contacts for electrons. Because of contact barriers and traps, injected holes accumulate in the film upon bias and are withdrawn when the bias is reversed; therefore, the lock-in detector is synchronized at the same frequency as the signal generator. However, since the contacts are symmetric, there is also a significant CA signal, albeit more noisy, at twice the modulation frequency. The frequency and voltage dependence of the charge injection depends on the quality of the electrode and intertube contacts as well as the density of intertube and intratube traps, but in the present work we are not concerned with a quantitative measure of the injected charge density.

One challenge in using the lock-in amplifier for modulation spectroscopy is determining the correct phase of the amplifier with respect to the signal generator. In order to unambiguously determine the phase in our system, we measured a series of absorption spectra in a Perkin-Elmer UV-Vis spectrometer with and without applied bias. Averaging 500 spectra over the region from 0.8 to 1.2 eV, we were able to discern a difference between field off and field on, proving that the applied field induces bleaching. The spectrometer was also used to obtain the absorption spectrum of our films (from which the derivative was calculated), and

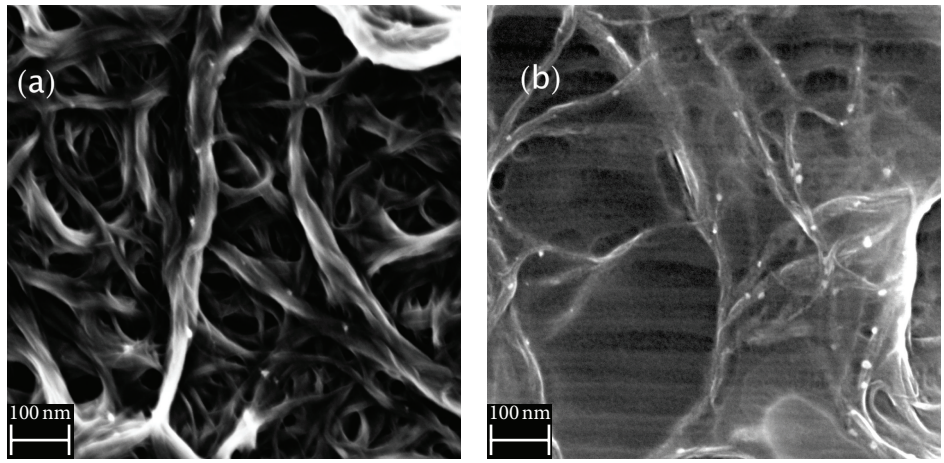

(a) (b)

Figure 2: SEM images of nanotube films used in this study. (a) Pure, conductive SWNT film used for CA. (b) Insulating SWNT composite with PVA used for EA. The bright flecks in the PVA composite image are thought to be PVA aggregates that did not fully dissolve during processing. The lower contrast and increased streaking in the PVA composite image are due to charging in the sample.

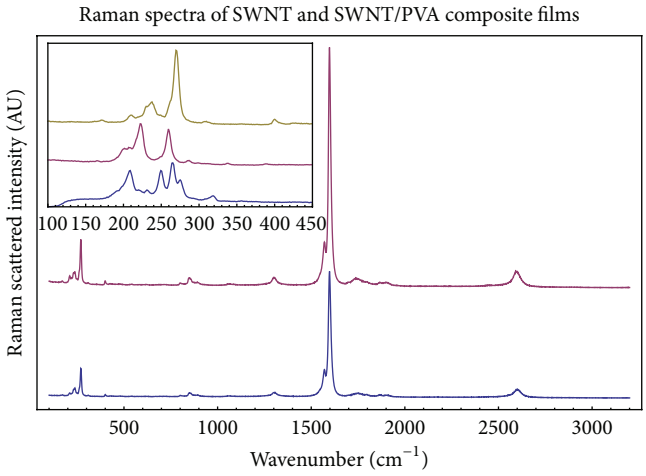

Figure 3: Raman spectra for pure SWNT film (lower) and SWNT-PVA composite (upper) obtained with 785 nm excitation. The two spectra are offset for clarity. No noticeable frequency shifts are observed. The inset shows the RBM modes obtained for 514 nm (bottom), 633 nm (middle), and 785 nm (upper) excitations, used to determine the diameters present in our samples.

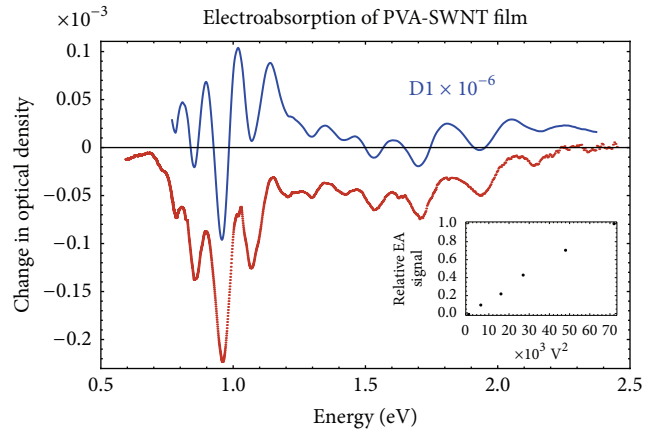

Figure 4: The change in absorption (red) of a PVA-SWNT composite film with an average field strength of 4×10^7 V/m shown with the calculated first derivative of the spectrum (blue, magnified). The inset shows the linear relationship between the EA signal at 1 eV and the applied field strength.

the π-plasmon background was subtracted using a 5th-order polynomial fit.

3. Results and Discussion

The electroabsorption of our nanotube film is shown in Figure 4 along with the calculated first derivative of the background-corrected absorption spectra. The features in the EA spectrum are quite similar to those in the first derivative, but there is an anomalous offset, most notably in the region of the spectrum around 1 eV where the lowest semiconducting exciton transitions lie. The electroabsorption signal scales linearly with the square of the field and has a strong polarization dependence with respect to the direction of the electric field as previously reported for electroabsorption in SWNTs.

To understand the nature of the offset, we measured CA on the same SWNTs, and the results are shown in Figure 5. Injected charges significantly screen excitons in semiconducting tubes while having little effect in conducting tubes where the carrier density is already relatively high; thus, the effect of injected charge is primarily to bleach the absorption of the semiconducting nanotubes. Figure 5 shows the spectral ranges corresponding to the first and second semiconducting transitions (S_{11} and S_{22}, resp.) and the first metallic transition (M_{11}) of nanotubes with an average diameter near 1.13 nm as determined by Raman spectroscopy.

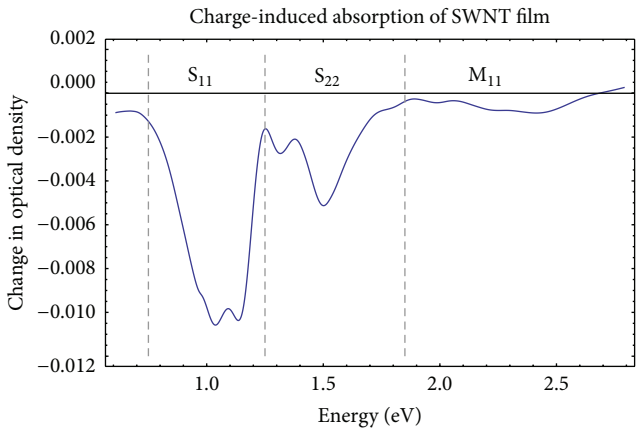

Figure 5: The CA spectrum with labels for the S_{11}, S_{22}, and M_{11} spectra regions. The primary influence of the injected charges is to bleach the semiconducting transitions while leaving the metallic transitions unaltered.

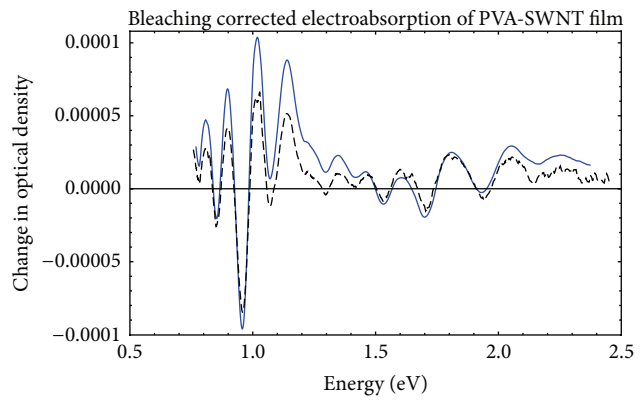

Figure 6: The adjusted EA spectrum (black, dashed) was obtained by removing the contribution from the CA using the fit parameters in Table 1 for (1). It is shown again with the calculated first derivative of the absorption (blue).

Table 1: A summary of the manually chosen fit parameters.

Parameter	Best fit value
Δp	6×10^{-18} eV m^2/V^2
m	0
f_{11}	0.131
f_{22}	0.032

These spectral ranges were determined from a Kataura plot [17] for pristine nanotubes since the PVA interacts weakly with the nanotubes and has an extremely low dielectric constant. The films are not dispersed enough for us to resolve and identify peaks corresponding to individual tubes, but rather the peaks comprise overlapping signals from small groups of tubes. Still, one can identify the spectral ranges corresponding to conglomerate peaks in the S_{11}, S_{22}, and M_{11} regions corresponding to nanotubes of this diameter.

The change in optical density for neutral excitations in an external electric field F is given by

$$-\frac{\Delta T}{T} \approx \Delta\alpha = \frac{1}{2}\Delta p F^2 \frac{\delta\alpha}{\delta E} + \frac{1}{6}(mF)^2 \frac{\delta^1\alpha}{\delta E^2} - F^2\delta f, \quad (1)$$

where p is the polarizability of the molecule, m is the dipole moment of the excited state, and δf is the contribution resulting from the transfer of oscillator strength from the unperturbed transitions to previously forbidden transitions [13]. Each of these terms is implicitly a function of the photon energy E, and in general δf is subject to the condition

$$\int_0^\infty \delta f dE = 0. \quad (2)$$

The only significant differences between the samples used for EA and CA measurements are the intertube connectivity and corresponding film conductivity, so we fit the EA spectrum to (1) by assuming that only the optically active singlet excitons contribute to the derivative-like signal and that the transfer term δf over the measured spectral range is entirely due to the charge-induced bleaching of the semiconducting transitions. We allow for differences in charge accumulation in the percolated, conductive film and the disperse, resistive film by taking the bleaching effect to be weakly frequency dependent. We approximate the transfer function as

$$\delta f = f_{11} \cdot S_{11} + f_{22} \cdot S_{22}, \quad (3)$$

where the f_n are constants and S_{11} and S_{22} are the components of the CA signal in those respective spectral regions. While the change in polarizability is different for different chirality tubes, we found a reasonable fit by using a single average value since the diameter distribution in our sample is relatively tight (0.93–1.3 nm). However, the actual determination of p depends on the value of F, which we have not established accurately. The bleaching corrected EA at an average applied field of 6×10^6 V/m is shown in Figure 6 along with the first derivative of the absorption. The fit parameters used to match the two spectra are given in Table 1.

4. Conclusions

There have been several studies of the EA spectra of nanotube films in the recent years, and each has measured different distributions of tube chiralities and different local environmental conditions. The extremely low dielectric constant and optical activity of PVA makes it an ideal matrix in which to obtain EA measurements on virtually pristine SWNTs [18]. We have shown that the EA signal in such films is a simple combination of a component proportional to the first derivative of the absorption and a component proportional to the charge-induced bleaching, with no need to include higher derivative terms or the notion of state mixing with lower lying "dark" excitons. This opens the door for refined calculations of exciton polarizability and therefore binding energy, using the relatively simple technique of electroabsorption if a suitable measurement or calculation of the actual field experienced by the nanotubes can be obtained.

We note the similarity between our analysis and the analysis of EA signals in conducting polymers, especially

the agreement with the photoexcited change in polarizability [13, 14]. However, unlike in polymer systems where multiple exciton manifolds exist, the good fit obtained while setting $m = 0$ suggests that the only result of the electrobleaching is the transfer of oscillator strength to transitions far from the exciton absorption energies. We have previously suggested that the oscillator strength goes to the free-carriers absorption because the injected charges increase the local carrier density [16]. Because the free-carriers absorption is so broad, the enhancement in the infrared absorption of SWNT films in this manner is expected to be small at any particular energy.

It is conceivable that scanning capacitance microscopy on the PVA-SWNT composite may help determine the potential distribution inside a biased film and allow for a more precise measure of F. Furthermore, if PVA-SWNT composites can be produced with individually dispersed SWNTs, or even tubes of a single chirality, then the average Δp we have obtained from our fit could be replaced with specific chirality-dependent values which would give greater insight into exciton binding energy variability among different tubes of similar diameter.

Conflict of Interests

The author declares that he has no competing interests.

Acknowledgments

The author thanks Dr. Tho Nguyen for his help in suggesting the charge-induced absorption experiment and Dr. Z. Valy Vardeny and Dr. Eugene Mishchenko for valuable discussion and assistance in interpreting the results. The author would especially like to acknowledge the Physics Department at the College of Charleston in Charleston, SC, USA, for allowing him the time to work on the analysis. Funding for this project was provided primarily by the Engineering Structures division at NASA Johnson Space Center.

References

[1] X. Calderon-Colon, H. Geng, B. Gao, L. An, G. Cao, and O. Zhou, "A carbon nanotube field emission cathode with high current density and long-term stability," *Nanotech-Nology*, vol. 20, no. 32, Article ID 325707, 2009.

[2] J. Wu, M. Wyse, D. McClain, N. Thomas, and J. Jiao, "Fabrication and field emission properties of triode-type carbon nanotube emitter arrays," *Nano Letters*, vol. 9, no. 2, pp. 595–600, 2009.

[3] S. Gupta, M. Hughes, A. H. Windle, and J. Robertson, "Charge transfer in carbon nanotube actuators investigated using in situ Raman spectroscopy," *Journal of Applied Physics*, vol. 95, no. 4, pp. 2038–2048, 2004.

[4] M. Musameh, M. R. Notivoli, M. Hickey et al., "Carbon nanotube webs: a novel material for sensor applications," *Advanced Materials*, vol. 23, no. 7, pp. 906–910, 2011.

[5] J. Di, D. Hu, H. Chen et al., "Ultrastrong, foldable, and highly conductive carbon nanotube film," *ACS Nano*, vol. 6, no. 6, pp. 5457–5464, 2012.

[6] P.-H. Wang, B. Liu, Y. Shen et al., "N-channel carbon nanotube enabled vertical field effect transistors with solution deposited ZnO nanoparticle based channel layers," *Applied Physics Letters*, vol. 100, no. 17, Article ID 173514, 2012.

[7] W. J. Kennedy, Z. V. Vardeny, S. Collins, R. H. Baughman, H. Zhao, and S. Mazumdar, "Electroabsorption spectroscopy of single walled nanotubes," http://arxiv.org/abs/cond-mat/0505071.

[8] H. Zhao and S. Mazumdar, "Elucidation of the electronic structure of semiconducting single-walled carbon nanotubes by electroabsorption spectroscopy," *Physical Review Letters*, vol. 98, no. 16, Article ID 166805, 2007.

[9] V. Perebeinos and P. Avouris, "Exciton ionization, Franz-Keldysh, and stark effects in carbon nanotubes," *Nano Letters*, vol. 7, no. 3, pp. 609–613, 2007.

[10] C. Gadermaier, E. Menna, M. Meneghetti, W. J. Kennedy, Z. V. Vardeny, and G. Lanzani, "Long-lived charged states in single-walled carbon nanotubes," *Nano Letters*, vol. 6, no. 2, pp. 301–305, 2006.

[11] H. Zhao, S. Mazumdar, C.-X. Sheng, M. Tong, and Z. V. Vardeny, "Photophysics of excitons in quasi-one-dimensional organic semiconductors: Single-walled carbon nanotubes and π -conjugated polymers," *Physical Review B*, vol. 73, no. 7, Article ID 075403, 2006.

[12] H. Kishida, Y. Nagasawa, S. Imamura, and A. Nakamura, "Direct observation of dark excitons in micelle-wrapped single-wall carbon nanotubes," *Physical Review Letters*, vol. 100, no. 9, Article ID 097401, 2008.

[13] S. J. Martin, D. D. C. Bradley, P. A. Lane, H. Mellor, and P. L. Burn, "Linear and nonlinear optical properties of the conjugated polymers PPV and MEH-PPV," *Physical Review B*, vol. 59, no. 23, pp. 15133–15142, 1999.

[14] P. J. Brewer, A. J. deMello, J. C. deMello et al., "Influence of carrier injection on the electromodulation response of trap-rich polymer light-emitting diodes," *Journal of Applied Physics*, vol. 99, Article ID 114502, 2006.

[15] J. Lee, B.-L. Lee, J. H. Kim, S. Lee, and S. Im, "Photoexcited charge collection spectroscopy of two-dimensional polaronic states in polymer thin-film transistors," *Physical Review B*, vol. 85, no. 4, Article ID 045206, 2012.

[16] W. J. Kennedy and Z. V. Vardeny, "The effects of charge injection in single-wall carbon nanotubes studied by charge-induced absorption," *Applied Physics Letters*, vol. 98, no. 26, Article ID 263110, 2011.

[17] A. Jorio, P. T. Araujo, S. K. Doorn, S. Maruyama, H. Chacham, and M. A. Pimenta, "The Kataura plot over broad energy and diameter ranges," *Physica Status Solidi B*, vol. 243, no. 13, pp. 3117–3121, 2006.

[18] M. H. Harun, E. Saion, A. Kassim, E. Mahmud, M. Y. Hussain, and I. S. Mustafa, "Dielectric properties of poly (vinyl alcohol)/polypyrrole composite polymer films," *Journal for the Advancement of Science and Arts*, vol. 1, no. 1, pp. 9–16, 2009.